Acta Crystallographica Section F
Structural Biology and Crystallization Communications
ISSN 1744-3091

Crystallization and preliminary X-ray crystallographic analysis of DNA gyrase GyrB subunit from *Xanthomonas oryzae* pv. *oryzae*

Ha Yun Jung,[a] Ki Jeung Lee,[a] Kyung Ha Kim,[a] Ji Hye Hyoung,[a] Mi Ra Han,[a] Hyun Kyoung Kim,[a] Lin-Woo Kang,[b] Yeh-Jin Ahn[c] and Yong-Seok Heo[a]*

[a]Department of Chemistry, Konkuk University, Hwayang-dong, Gwangjin-gu, Seoul 143-701, Republic of Korea, [b]Department of Advanced Technology Fusion, Konkuk University, Hwayang-dong, Gwangjin-gu, Seoul 143-701, Republic of Korea, and [c]Department of Life Science, College of Natural Sciences, Sangmyung University, 7 Hongji-dong, Jongno-gu, Seoul 110-743, Republic of Korea

Correspondence e-mail: ysheo@konkuk.ac.kr

Received 9 October 2009
Accepted 11 November 2009

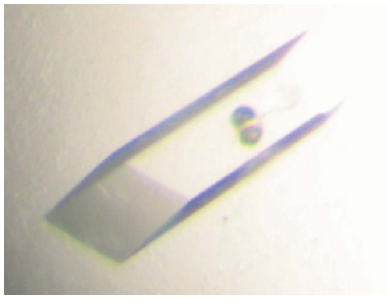

DNA gyrase is a type II topoisomerase that is essential for chromosome segregation and cell division owing to its ability to modify the topological forms of bacterial DNA. In this study, the N-terminal fragment of the GyrB subunit of DNA gyrase from *Xanthomonas oryzae* pv. *oryzae* was overexpressed in *Escherichia coli*, purified and crystallized. Diffraction data were collected to 2.10 Å resolution using a synchrotron-radiation source. The crystal belonged to space group $I4_1$, with unit-cell parameters $a = b = 110.27$, $c = 70.75$ Å. The asymmetric unit contained one molecule, with a V_M of 2.57 Å^3 Da^{-1} and a solvent content of 50.2%.

1. Introduction

Bacterial blight disease has become a major disease of rice in Asian countries in the last three decades (Ezuka & Kaku, 2000). *Xanthomonas oryzae* pv. *oryzae* is a Gram-negative rod-shaped bacterium that causes bacterial blight. Rice plants become wilted if infection occurs during the seedling or early tillering stages. When infection occurs in later stages, leaf-blight lesions enlarge in length and width and gradually turn from greyish green to chlorotic (Mew, 1993). During infection, *X. oryzae* pv. *oryzae* employs diverse tools to overcome the host innate defence system, resulting in blight disease. Bacterial blight is a vascular disease in which *X. oryzae* pv. *oryzae* grows and colonizes the xylem vessels, eventually clogging them; several virulence-associated determinants have been found, including exopolysaccharide production, hypersensitive response and pathogenicity (*hrp*) genes (Cho *et al.*, 2008; Shen & Ronald, 2002). Although bacterial blight is the most important rice disease from an economic point of view, there are currently no effective antibacterial agents against *X. oryzae* pv. *oryzae*.

DNA gyrase is a bacterial type II topoisomerase that introduces supercoils into DNA (Reece & Maxwell, 1991). DNA gyrase, which is encoded by *gyrA* and *gyrB*, forms an A_2B_2 tetramer and the B subunit (GyrB) contains an ATPase active site in the N-terminal domain (43 kDa), which is referred to as the ATP-operating clamp (Maxwell & Lawson, 2003). Upon ATP binding, this clamp closes by dimerization of the N-terminal domain, trapping the T-segment of the DNA. The C-terminal domain of GyrB is involved in interaction with the GyrA subunit and the DNA substrate. DNA gyrase is the target of two antibiotic families: the coumarins, such as novobiocin, and the quinolones, such as ciprofloxacin, sparfloxacin and grepafloxacin (Anderson *et al.*, 1998; Hardy & Cozzarelli, 2003). The coumarins are ATP-competitive inhibitors of the enzyme and the quinolones form a ternary complex with the enzyme in the presence of DNA. To date, crystal structures of the N-terminal domains of the GyrB subunits from *Escherichia coli* and *Thermus thermophilus* have been described (Brino *et al.*, 2000; Lamour *et al.*, 2002). These structures were similar to the known topoisomerase IV ParE subunit, with similar functions and a high homology in their amino-acid sequences (Bellon *et al.*, 2004). To provide further structural data regarding the catalytic mechanism of DNA gyrase and to facilitate the discovery of effective antibacterial agents against *X. oryzae* pv. *oryzae*, we have crystallized

and performed X-ray crystallographic experiments on the N-terminal domain of the DNA gyrase GyrB subunit from *X. oryzae* pv. *oryzae*.

2. Materials and methods

2.1. Cloning, protein expression and purification

The gene encoding the N-terminal fragment (amino acids 76–463) of the GyrB subunit was amplified from bacterial cells of *X. oryzae* pv. *oryzae* strain KACC10331 by the polymerase chain reaction (PCR) using specific primers that were designed based on the published genome sequence (Lee *et al.*, 2005). The forward primer contained an *Nde*I restriction site (shown in bold) and had the sequence 5′-CCC CCC **CAT ATG** GAC TCC AGC AAG ATC ACC GTG-3′, while the reverse primer contained a *Bam*HI site (shown in bold) and had the sequence 5′-CCC CCC **GGA TCC** TCA GCG GGT GAG GTC GCG CGC CT-3′. The PCR product was then subcloned between the *Nde*I and *Bam*HI sites of pET-15b vector (Novagen, USA). This construct contained a hexahistidine tag and a thrombin cleavage site (MGSSHHHHHHSSGLVPRGSH) at the N-terminus for purification purposes. The GyrB/pET-15b plasmid was transformed into *Escherichia coli* BL21 (DE3) strain (Novagen) and the cells were grown in a shaking incubator at 310 K in LB broth medium supplemented with 50 µg ml^{-1} ampicillin. Protein expression was induced by adding 0.5 m*M* isopropyl *β*-D-1-thiogalactopyranoside (IPTG) when the cells reached an optical density at 600 nm of about 0.6 and the cells were cultured at the same temperature for an additional 4 h. The cultured cells were harvested by centrifugation at 3000*g* for 30 min at 277 K. The cell pellet was resuspended in binding buffer (20 m*M* Tris pH 8.0, 100 m*M* NaCl and 20 m*M* imidazole) and disrupted by sonication at 277 K. The crude lysate was centrifuged at 25 000*g* for 1 h at 277 K. The supernatant was then loaded onto an Ni^{2+}-chelated HisTrap FF crude column (GE Healthcare, USA) which had been pre-equilibrated with binding buffer. The protein was eluted with elution buffer (20 m*M* Tris pH 8.0, 100 m*M* NaCl and 400 m*M* imidazole). The eluted protein was treated with thrombin overnight at 277 K to remove the hexahistidine tag from the recombinant protein. After thrombin cleavage, the protein was concentrated and purified by gel-filtration chromatography on a Superdex 200 16/60 column (GE Healthcare, USA) which had been pre-equilibrated with buffer containing 20 m*M* Tris pH 8.0 and 100 m*M* NaCl. The purified protein was concentrated to 15 mg ml^{-1} in the gel-filtration buffer and the homogeneity of the purified protein was examined by 12% SDS–PAGE and determined to be >95%.

2.2. Crystallization and data collection

As we failed to crystallize the apo form of the protein, we added 5′-adenylyl *β*,*γ*-imidodiphosphate (ADPNP) and Mg^{2+} to the concentrated protein solution to give an ADPNP:Mg^{2+}:protein molar ratio of 5:10:1 and incubated the mixture for 1 h at 277 K. Crystallization of the incubated protein was initiated by crystal screening at 293 K using a Hydra II e-drop automated pipetting system (Matrix Technologies Ltd, UK) using 96-well sitting-drop Intelli-Plates (Art Robbins Instruments, USA) with drops consisting of 400 nl protein solution and 400 nl well solution and equilibrating over 70 µl well solution. Commercial screening kits from Hampton Research were used in the preliminary screening. Initial crystals were obtained under the condition 0.1 *M* bis-tris pH 6.5, 25%(*w*/*v*) polyethylene glycol 3350. This crystallization condition was further optimized by the hanging-drop vapour-diffusion method using 24-well VDX plates (Hampton Research, USA) at 293 K. The drops used in the optimized crystallization condition were prepared by mixing 1.0 µl protein solution with 1.0 µl reservoir solution (0.1 *M* sodium cacodylate pH 6.8, 22% polyethylene glycol 3350). Each hanging drop was positioned over 500 µl reservoir solution. Suitable-sized crystals (Fig. 1) were obtained within 5 d and were cryoprotected by soaking for 3 s in cryoprotectant solution containing 0.1 *M* sodium cacodylate pH 6.8, 22% polyethylene glycol 3350 and 25%(*v*/*v*) glycerol and were flash-frozen in liquid nitrogen. They were then mounted on the goniometer in a stream of cold nitrogen at 100 K. X-ray diffraction data were collected from a cooled crystal using an ADSC Quantum CCD 210 detector on beamline 6B at Pohang Light Source (PLS), Republic of Korea. A total range of 180° was covered with 1.0° oscillation and 15 s exposure per frame. The wavelength of the synchrotron X-ray beam was 1.0000 Å and the crystal-to-detector distance was set to 160 mm. X-ray diffraction data were collected to 2.10 Å resolution (Fig. 2).

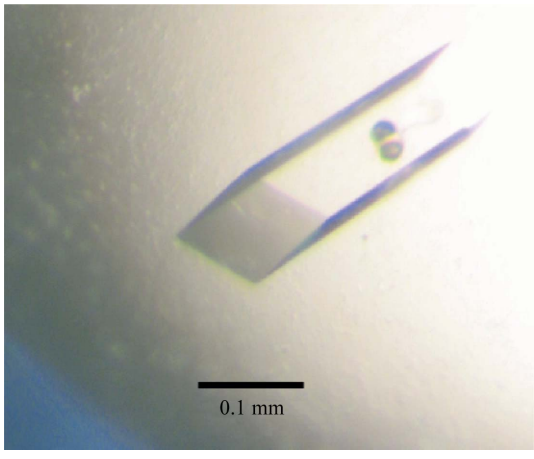

Figure 1
A crystal of the N-terminal fragment of the GyrB subunit from *X. oryzae* pv. *oryzae* grown in 0.1 *M* sodium cacodylate pH 6.8, 22% polyethylene glycol 3350.

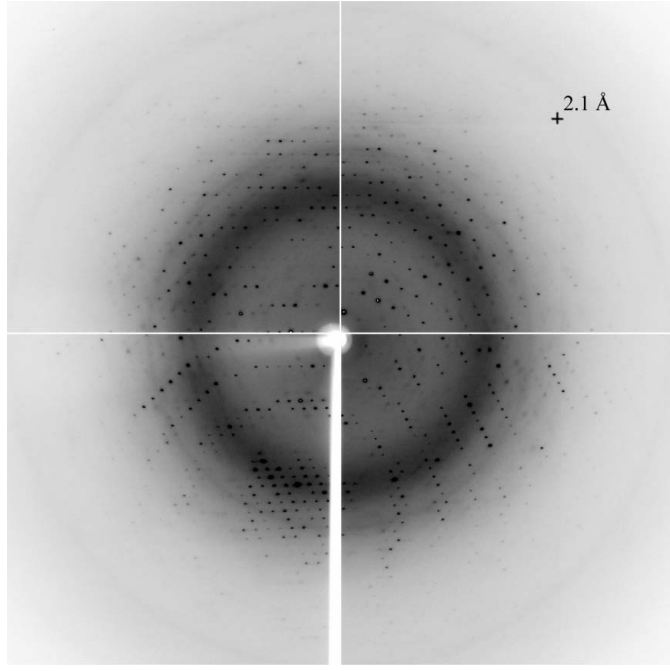

Figure 2
Diffraction image of the GyrB crystal. The resolution limit (2.1 Å) is indicated.

Table 1
Data-collection statistics.

Values in parentheses are for the last resolution shell.

Synchrotron	PLS, beamline 6B
Wavelength (Å)	1.0000
Resolution range (Å)	50.0–2.10 (2.14–2.10)
Space group	$I4_1$
Unit-cell parameters (Å)	
$a = b$	110.27
c	70.75
Total No. of reflections	178025
No. of unique reflections	24754
Redundancy	7.2 (6.3)
Completeness (%)	99.6 (100.0)
Molecules per ASU	1
V_M (Å^3 Da^{-1})	2.57
Solvent content (%)	50.2
Average $I/\sigma(I)$	45.6 (4.7)
R_{merge}† (%)	5.3 (41.5)

† $R_{merge} = \sum_{hkl}\sum_i |I_i(hkl) - \langle I(hkl)\rangle| / \sum_{hkl}\sum_i I_i(hkl)$, where $I_i(hkl)$ is the intensity of an individual reflection hkl and $\langle I(hkl)\rangle$ is the average intensity of reflection hkl.

Data were indexed, integrated, scaled and averaged using the *HKL*-2000 software package (Otwinowski & Minor, 1997).

3. Results and discussion

The N-terminal fragment (amino acids 76–463) of the GyrB subunit from *X. oryzae* pv. *oryzae* was cloned, expressed, purified and crystallized for structural study. X-ray diffraction data from the crystal indicated that the crystal belonged to space group $I4_1$ on the basis of systematic absences, with unit-cell parameters $a = b = 110.27$, $c = 70.75$ Å. Data-collection statistics are provided in Table 1. According to Matthews coefficient calculations, the crystallographic structure contains only one monomeric unit in the asymmetric unit, with a V_M of 2.57 Å^3 Da^{-1} and a solvent content of 50.2% (Matthews, 1968). The structure solution obtained by the molecular-replacement (MR) method using the *CNS* package (Brünger *et al.*, 1998) using the crystal structure of *E. coli* GyrB (PDB code 1ei1) as a model made it clear that the asymmetric unit of the crystal contained one protein molecule. The best MR solution was obtained using one monomer of the dimeric structure of *E. coli* GyrB as a template, giving an *R* factor of 44.6% for data in the resolution range 20–3.5 Å. This final model is currently being refined and the structural details will be described in a separate paper.

We thank Dr K. H. Kim at beamline 6B, Pohang Light Source (PLS) for her assistance. This work was supported by a grant (Code No. 20070501034003) from the BioGreen 21 Program, Rural Development Administration, South Korea and by the Korea Research Foundation Grant funded by the Korean Government (MOEHRD; KRF-2007-313-C00621).

References

Anderson, V. E., Gootz, T. D. & Osheroff, N. (1998). *J. Biol. Chem.* **273**, 17879–17885.
Bellon, S., Parsons, J. D., Wei, Y., Hayakawa, K., Swenson, L. L., Charifson, P. S., Lippke, J. A., Aldape, R. & Gross, C. H. (2004). *Antimicrob. Agents Chemother.* **48**,1856–1864.
Brino, L., Urzhumtsev, A., Mousli, M., Bronner, C., Mitschler, A., Oudet, P. & Moras, D. (2000). *J. Biol. Chem.* **275**, 9468–9475.
Brünger, A. T., Adams, P. D., Clore, G. M., DeLano, W. L., Gros, P., Grosse-Kunstleve, R. W., Jiang, J.-S., Kuszewski, J., Nilges, M., Pannu, N. S., Read, R. J., Rice, L. M., Simonson, T. & Warren, G. L. (1998). *Acta Cryst.* D**54**, 905–921.
Cho, H. J., Park, Y. J., Noh, T. H., Kim, Y. T., Kim, J. G., Song, E. S., Lee, D. H. & Lee, B. M. (2008). *Microb. Pathog.* **44**, 473–483.
Ezuka, A. & Kaku, H. (2000). *Bull. Natl Inst. Agrobiol. Resour. (Jpn)*, **15**, 53–54.
Hardy, C. D. & Cozzarelli, N. R. (2003). *Antimicrob. Agents Chemother.* **47**, 941–947.
Lamour, V., Hoermann, L., Jeltsch, J. M., Oudet, P. & Moras, D. J. (2002). *J. Biol. Chem.* **277**, 18947–18953.
Lee, B. M. *et al.* (2005). *Nucleic Acids Res.* **33**, 577–586.
Matthews, B. W. (1968). *J. Mol. Biol.* **33**, 491–497.
Maxwell, A. & Lawson, D. M. (2003). *Curr. Top. Med. Chem.* **3**, 283–303.
Mew, T. W. (1993). *Xanthomonas*, edited by J. G. Swings & E. L. Civerolo, pp. 30–40. London: Chapman & Hall.
Otwinowski, Z. & Minor, W. (1997). *Methods Enzymol.* **277**, 307–326.
Reece, R. J. & Maxwell, A. (1991). *CRC Crit. Rev. Biochem. Mol. Biol.* **26**, 335–375.
Shen, Y. & Ronald, P. (2002). *Microbes Infect.* **4**, 1361–1367.